JOURNAL OF OPTOELECTRONICS AND ADVANCED MATERIALS Vol. 9, No. 11, November 2007, p. 3546 - 3548

Six-month ground-based water vapour Raman lidar measurements over Athens, Greece and system validation

R. E. MAMOURI[a*], A. PAPAYANNIS[a], G. TSAKNAKIS[a], V. AMIRIDIS[b]
[a]*National Technical University of Athens, Physics Department, Laser Remote Sensing Laboratory, Heroon Polytechniou 9, 15780 Zografou, Greece*
[b]*Institute for Space Applications and Remote Sensing, National Observatory of Athens, Palaia Penteli, Greece*

Water vapour is one of the most important greenhouse gases, since it causes about two third of the natural greenhouse effect of the Earth's atmosphere. To improve the understanding of the role of the water vapour in the atmosphere, extensive water vapour profiles with high spatio-temporal resolution are therefore necessary. A ground-based Raman lidar system is used to perform water vapour measurements in Athens, Greece (37.9^{o}N, 23.6^{o}E, 200 m asl.). Water vapour mixing ratio measurements are retrieved from simultaneous inelastic H_2O and N_2 Raman backscatter lidar signals at 387 nm (from atmospheric N_2) and 407 nm (from H_2O). Systematic measurements are performed since September 2006. A new algorithm is used to retrieve water vapour vertical profiles in the lower troposphere (0.5-5 km range height asl.). The lidar observations are complemented with radiosonde measurements. Radiosonde data are obtained daily (at 00:00 UTC and 12:00 UTC) from the Hellenic Meteorological Service (HMS) of Greece which operates a meteorological station at the "Hellinikon" airport (37. 54^o N, 23.44^o E, 15m asl) in Athens, Greece. First results of the systematic intercomparison between water vapour profiles derived simultaneously by the Raman lidar and by radiosondes are presented and discussed.

(Received August 1, 2007; accepted November 1, 2007)

Keywords: Raman LIDAR, Water vapour measurements

1. Introduction

Water vapour is the most influential greenhouse gas, since it absorbs infrared radiation emitted from Earth's surface and lower atmosphere more than any other constituent, thereby causing about two third of the natural greenhouse effect of the Earth's atmosphere (Forster, et al., 2007). Moreover, the water vapour vertical and horizontal distribution is characterized by a strong spatial and temporal variability which is generally strongly influenced by the large-scale atmospheric circulation (i.e. front movement, stratosphere to troposphere exchange processes) and local convection phenomena.

To improve the understanding of the role that water vapour has in weather and climate prediction and test global warming models, extensive and systematic water vapour profiles obtained with high spatio-temporal resolution are therefore required.

Lidars have been used to obtain the water vapour vertical profiles not only in the lower troposphere (where the water vapour field presents an enhanced spatial and temporal variability which cannot be followed by infrequent radiosonde launches) but also in the whole free troposphere since the 1960s (Melfi, 1972, Whiteman, 2003, Ansmann et al. 1992, Ferrare, et al., 1995). In particular, the Raman lidar technique is the most suitable one to obtain, simultaneously, independent vertical profile measurements of water vapour and aerosol optical properties in the troposphere (Ansmann et al., 1992).

2. Experimental setup

2.1 System description

One of the main purposes of the NTUA Raman lidar is the measurement of the mixing ratio of water vapour to dry air during nighttime. The lidar system is based on a frequency tripled Nd:YAG laser, witch emits pulses of 75 mJ output energy at 355 nm, with a 10 Hz repetition rate. The optical receiver is a Cassegrainian reflecting telescope with a primary mirror of 300 mm diameter and of focal length f=600 mm, directly coupled, through an optical fiber, to the lidar signal multi-channel detection box. The PMT detectors used, are operated both in the analog and photon-counting mode and the spatial raw resolution of the detected signals is 15 m.

The elastically backscattered lidar signal at 355 nm is detected both in the analogue and photon-counting mode, while the inelastically backscattered Raman signals by N_2 at 387 nm and by H_2O at 407 nm are detected only in the photon-counting mode. Narrow-band interference filters (IF) are used to suppress the atmospheric background noise at the detected wavelengths. Table 1 presents the Full-Width-at-Half-Maximum (FWHM) and the corresponding transmission of the interference filters used.

Table 1. FWHM and corresponding transmission of the IF filters used.

Wavelength (nm)	FWHM (nm)	Transmission (%)
355	3	50
387 and 407	3	60

2.2 Methodology

Raman lidars can measure the mixing ratio of water vapour to dry air. This technique has been developed for nighttime observations (Melfi, 1972; Ansmann et al., 1992). The water vapour mixing ratio is obtained from the measurement of the water vapour to reference signal ratio

$P_{\lambda_{H_2O}(z)} / P_{\lambda_{ref}(z)}$, where the reference gas is either oxygen or nitrogen. Using two Raman lidar equations for the wavelengths λ_{H_2O} and λ_{N_2}, forming the signal ratio, and rearranging the resulting equation, the mixing ratio is obtained as

$$m(z) = K_m \frac{P_{\lambda_{H_2O}(Z)}}{P_{\lambda_{N_2}(Z)}} \times \frac{\exp\{-\int_o^z [\alpha^{aer}_{\lambda_{N_2}}(\xi) + \alpha^{mol}_{\lambda_{N_2}}(\xi)]d\xi\}}{\exp\{-\int_o^z [\alpha^{aer}_{\lambda_{H_2O}}(\xi) + \alpha^{mol}_{\lambda_{H_2O}}(\xi)]d\xi\}} \quad (1)$$

The overall system constant $K_m = K_{\lambda_{N_2}} / K_{\lambda_{H_2O}}$ can in principle be deduced from the known Raman cross sections and the measured properties of the spectrometer used, but in practice it is determined from the comparison of the lidar measurement with critically evaluated data from a radiosonde ascent. In the calculation of the transmission ratio, Rayleigh scattering and aerosol extinction have to be considered. Other extinction contribution as ozone absorption can be neglected. The reduction in transmission due to Rayleigh scattering is determined from a standard atmosphere model fit to measured ground level values of temperature and pressure, or from radiosonde data when available. The effect of the particle optical thickness is estimated from extinction coefficients derived from the Raman signal profile of the reference gas (nitrogen). The effect of the particle extinction is negligible on the mixing ratio determination under clear air conditions but must be taking into account if an optically dense medium like a water cloud is present.

A new algorithm for real-time lidar signal processing was developed offering also the possibility of applying different digital filters in order to retrieve water vapour mixing ratio profiles with low uncertainties, especially in the lower troposphere where the small amounts of water vapour content require a careful data analysis. The detailed inversion procedure has been previously described by Whiteman et al. (2003).

3. System Calibration- results and discussion

Since September 2006 the NTUA Raman lidar system over Athens, Greece, measures the vertical profiles of the water vapour mixing ratio. In Fig. 1 a typical example for 13 September 2006, of time series of heights profile of the water vapour-dry air mixing ratio and the vertical profile of the same magnitude, is presented. One can see increased values of water vapour mixing ratio (a localised humid layer) at the height range of 3500-4000 m.

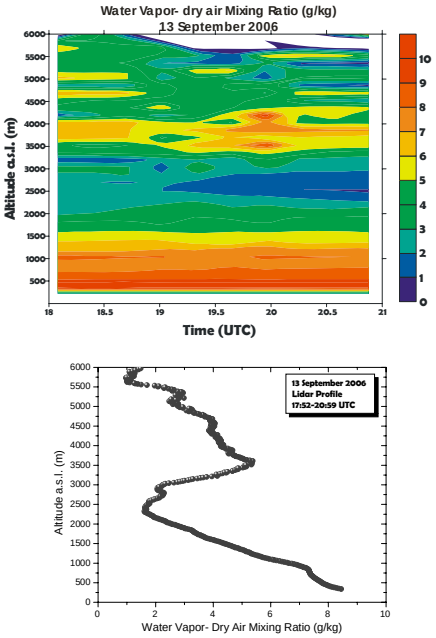

Fig. 1. Water vapour - dry air mixing ratio time series obtained by the NTUA Raman lidar on 13 September 2006. Temporal and vertical resolutions are 12 minutes, and 15 meters, resepctively (left). Water vapour - dry air mixing ratio vertical profile obtained by the NTUA Raman lidar on 13 September 2006. The average values were obtained over the time period from 17:52 to 20:59 UTC.

The Raman lidar must be calibrated before it is used for retrieval of the meteorological parameters. The lidar calibration coefficient K_m is determined from the radiosonde- lidar comparisons.

The NTUA Raman lidar system has been calibrated through systematic direct intercomparisons in the 0.5-2.5 km height region asl., with simultaneously launched radiosondes obtained at the "Hellinikon" airport (37. 54^o N, 23.44^o E, 15m asl) in Athens, Greece. Figure 2 illustrates the determination of the constant K_m. Figure 2a presents the ratio of the water vapour mixing ratio profile acquired with a radiosonde to that calculated from the ratio of the water vapour to the nitrogen lidar return by Eq. (1) with K_m=1. The height variations of the calibration constant K_m could be explained by temporal changes in the vertical distribution of the moisture during the measurements (Mattis et al., 2002).

Such an example of intercomparison (180-min Raman water vapour profile) is shown in Fig. 2b (January 26, 2007). The radiosonde was launched at 00:04 UTC. The lidar profile is an average over the time period from 00:47 to 03:14 UTC. We have used the entire profile presented in figure to calculate the mean value of lidar calibration coefficient K_m and to estimate the standard deviation ΔK_m. The profile of the water vapour to dry air mixing ratio presented in Fig. 2b has been calculated on the basis of the mean value of the constant.

Seventeen lidar-radiosonde comparisons have been made since September 2006. The variations in the

calibration coefficient were found to be close to 4%. The mean value of the calibration constant for the seventeen cases of our study is 80.7 ± 5.2. Each Raman lidar water vapour profile is an average of 180 minutes. Every file is based on about 4000 laser shots emitted within 6 minutes at a pulse repetition rate of 10 Hz.

From the analysis of the seventeen systematic intercomparison data we have calculated the difference percentage between water vapour profiles derived simultaneously by the Raman lidar and by radiosondes. This analysis showed that under most meteorological conditions, the statistical error in the retrieved 180-min water vapour profile by the Raman lidar remains less than 8% up to 1500 m and is about 20% for heights $\geq$ 2500 m Fig. 3. The value of the water vapour error increases in height ranges with strong backscattering witch is usually water clouds. These layers were mostly present in heights under 3000 m for Athens and for the specific cases that we are examining here.

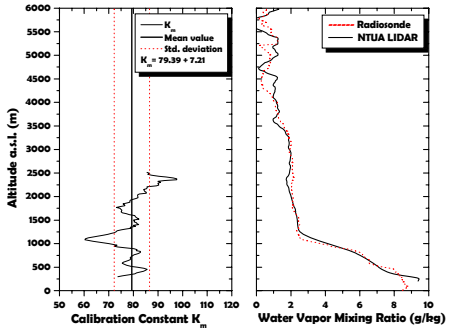

Fig. 2. (a) Calibration constant K_m defined as the Ratio of the water vapour mixing ratio measured with the radiosonde and that obtained with an uncalibrated lidar. (b), Mixing ratio measured with radiosonde and determined with a calibrated Raman lidar (K_m= 79.39). The lidar signals were smoothed before calculation of the mixing ratio to reduce signal noise.

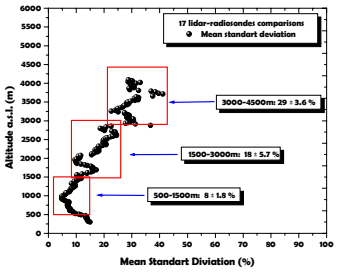

Fig. 3. Relative difference (%) between the water vapour profiles derived by the Raman lidar and radiosondes for 17 cases.

3. Conclusions

Since September 2006 NTUA Raman lidar system performs systematic measurements of water vapour mixing ratio. Simultaneously acquired inelastic H_2O and N_2 Raman backscatter lidar signals at 387 nm and 407 nm retrieve the water vapour – dry air mixing ratio.

In this study seventeen lidar radiosonde comparisons were performed. The statistical analysis of seventeen cases showed that the variation in the calibration coefficient K_m is about 4%. The height variations of the calibration constant, witch found to be close to 10%, attributed to temporal changes in vertical distribution of moisture during the measurements.

The intercomparisons showed that under most meteorological conditions, the absolute difference between water vapour profile retrieved by the Raman lidar and correspondent radiosonde generally remains less than 10%. The relative statistical error increases above layers with strong backscattering.

Acknowledgements

The project PENED 2003 is co-financed 75% of public expenditure through EC - European Social Fund and 25% of public expenditure through Ministry of Development, General Secretariat of Research and development (Project 03-ED-169) and through private sector (Raymetrics SA.), under Measure 8.3 of OPERATIONAL PROGRAMME "COMPETITIVE-NESS" in the 3rd Community Support Programme. The radiosonde data were provided by the Hellenic Meteorological Service (HMS).

References

[1] A. Ansmann, M. Riebesell, U. Wandinger, C. Weitkamp, E. Lahmann, W. Michaelis, Applied Physics **B55**, 18-28 (1992).

[2] Forster, P., V. Ramaswamy, P. Artaxo, T. Berntsen, R. Betts, D.W. Fahey, J. Haywood, J. Lean, D.C. Lowe, G. Myhre, J. Nganga, R. Prinn, G. Raga, M. Schulz and R. Van Dorland (2007), Changes in Atmospheric Constituents and in Radiative Forcing. /In: Climate Change 2007: The Physical Science Basis. Contribution of Working Group I to the Fourth Assessment Report of the Intergovernmental Panel on Climate Change /[Solomon, S., D. Qin, M. Manning, Z. Chen, M. Marquis, K.B. Averyt, M.Tignor and H.L. Miller (eds.)]. Cambridge University Press, Cambridge, United Kingdom and New York, NY, USA.

[3]R.A. Ferrare, S.H. Melfi, D.N. Whiteman, K.D. Evans, F.J. Schmidlin, and D.O'C. Starr, Journal of Oceanic and Atmospheric Technology **12,** 1177–1195 (1995).

[4] I. Mattis, A. Ansmann, D. Althausen, V. Jaenish, U. Wandinger, D. Muller, Y. Arshinov, S. Bobrovnikov, Y. Serikov, Applied Optics **41**, 6451-6462 (2002).

[5] S. H. Melfi, Applied Optics **11**, 1605–1610 (1972).

[6] D. N. Whiteman, S. H. Melfi, R. A. Ferrare, Applied Optics **31**, 3068–3081 (1992).

[7] D. N. Whiteman, Applied Optics **42**, 2593-2608 (2003).

*Corresponding author: rmamouri@central.ntua.gr

JOURNAL OF OPTOELECTRONICS AND ADVANCED MATERIALS Vol. 9, No. 11, November 2007, p. 3546 - 3548